

SIMS INVESTIGATION OF FURNACE-BAKED Nb

E.M. Lechner^{†1}, J.W. Angle², F.A. Stevie³, M.J. Kelley^{1,2}, C.E. Reece¹, and A.D. Palczewski¹

¹Thomas Jefferson National Accelerator Facility, Newport News, VA, USA

²Virginia Polytechnic Institute and State University, Blacksburg, VA, USA

³Analytical Instrumentation Facility, North Carolina State University, Raleigh, NC, USA

Abstract

Impurity-alloying SRF cavities via thermal diffusion has yielded highly efficient Nb resonators. Recently, SRF cavities vacuum heat treated at 300 – 400 °C for a few hours have exhibited high quality factors and behavior typical of alloyed cavities. Using secondary ion mass spectrometry, we investigated the interstitial concentration of carbon, nitrogen, and oxygen in niobium prepared by this method. Our investigation shows that oxygen is likely the primary diffusant in such recipes and is well-described by Ciovati's model for native niobium oxide dissolution and oxygen diffusion.

INTRODUCTION

Recently, Ito [1] explored vacuum heat treating Nb SRF cavities between 200 °C and 800 °C. After vacuum heat treating the cavities for 3 hours in the temperature range of 300 °C to 400 °C, their RF tests showed a pronounced “anti-Q-slope” (decreasing surface resistance with increasing field), extremely high quality factors, and reduced quench fields, which are all typical qualities previously associated with nitrogen-alloyed Nb cavities. In Ito's work, oxygen diffusion from the native Nb oxide was assumed to be the alloying mechanism. Recent works performed at Fermi National Accelerator Laboratory (FNAL) are extremely similar to the vacuum heat treatments of Ito where cavities were first vacuum heat-treated, in some cases exposed to nitrogen, and RF tested without exposure to atmosphere [2, 3]. FNAL's time-of-flight secondary ion mass spectrometry (TOF-SIMS) measurements observed Nb₂O₅ dissolution and a qualitative increase in nitrogen concentration near the surface ~10 nm deep. From these observations it was assumed that nitrogen was the primary alloying diffusant. In both works, the cavities did not require the injection of gases or post heat treatment chemistry to yield the high quality factors.

Our recent SIMS investigation [4] found elevated oxygen content near the surface of samples prepared in the similar way as Ito [1]. RF measurements of a Nb SRF cavity prepared via vacuum heat treatment at 300 °C and subsequently electropolished 180 nm to exclude any ingress of C and N demonstrated that the enhancement in quality factor is mainly due to interstitial oxygen alloying via a thermal diffusion process. The measurements made in [4] found that the thermal diffusion process was con-

sistent with Ciovati's model [5] of Nb₂O₅ dissolution and oxygen diffusion.

EXPERIMENTAL

Nb samples were prepared following a similar process to Ito [1]. Samples were cut from Tokyo Denkai ASTM 6 Nb stock procured using the XFEL/007 specification. First the stock was vacuum annealed at 900 °C to promote grain growth following the same procedure as the 1.3 GHz single-cell cavity, SC-11 used for RF validation. Samples were first nano-polished (NP) by a vendor to provide sufficiently flat samples for SIMS measurements. After the nano-polish, the samples underwent a 600°C/10hr heat-treatment to remove hydrogen introduced by the mechanical polishing. Subsequently samples underwent a 20 μm cold electropolish with the typical HF/H₂SO₄ solution [6]. During each heat treatment, samples were housed in a double-walled Nb foil container to minimize any furnace contamination [7]. To investigate the parameter space of the diffusion process, samples were baked for various times and temperatures.

A CAMECA 7f Geo magnetic sector SIMS instrument was used to acquire dynamic SIMS measurements. The primary ion beam is comprised of Cs⁺ ions with an impact energy of 8 keV. The ion beam is rastered over a 150 μm × 150 μm area with a data collection area of 63 μm × 63 μm centered inside the larger raster. Quantitation of the SIMS depth profiles was performed using implant standards [8]. The implant standards used here were dosed with C, N and O at 2×10¹⁵ atoms/cm² at 135 keV, 160 keV and 180 keV, respectively by Leonard Kroko Inc.

Shallow depth profiles found expected background concentrations [9] of C and N, but a large enhancement in oxygen content as shown in Fig. 1. Any ingress of C or N was minor in samples vacuum heat treated at 350 °C for 2.7 hours. In a process of vacuum heat treating Nb without a gaseous oxygen source, the ingress of oxygen is due to oxygen dissolution from the 3-6 nm thick native pentoxide rather than from oxygen pickup from the furnace environment [10-12]. An SRF cavity, SC-11, was subjected to a vacuum heat treatment at 320 °C for 1 hour using furnace caps [7] to confirm the effects of O alloying. Afterward, the heat treatment, the cavity underwent a high pressure rinsed before assembly for RF testing. RF measurements for SC-11 are shown in Fig. 2. Prior to O alloying, the cavity was high field Q slope limited. After the O alloying the cavity exhibited a pronounced “anti-Q-slope” with a maximum Q_0 of 4.6×10^{10} at 16 MV/m and

* Work supported by U.S. DOE Contract No. DE-AC05-06OR23177 and grant DE-SC0018918

† lechner@jlab.org

Content from this work may be used under the terms of the CC BY 4.0 licence (© 2022). Any distribution of this work must maintain attribution to the author(s), title of the work, publisher, and DOI

a quench field of 27 MV/m. This observed “anti-Q-slope” is due primarily to

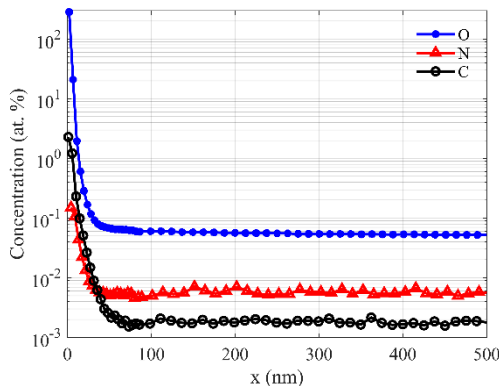


Figure 1: Typical calibrated SIMS depth profile of a sample vacuum heat treated at 350 °C for 2.7 hours presenting a large enhancement in oxygen with minor amounts of C and N.

the interstitial oxygen observed in our SIMS measurements which was confirmed by a cavity that underwent a shallow electropolish to remove any ingress of nitrogen or carbon in [4].

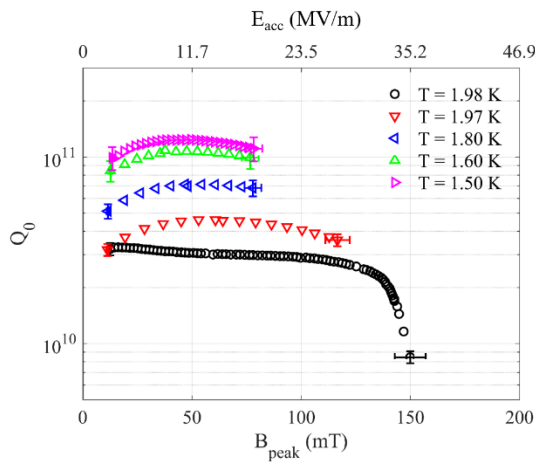


Figure 2: $Q_0(B_{peak})$ measurements for cavity SC-11 after a 40 μ m electropolish in black and after vacuum furnace heat treatment at 315 °C for 1 hour in blue, magenta, green and red at several temperatures.

PREDICTION OF ALLOYING TIMES AND TEMPERATURES

In [4] we showed that this process is well described by Ciovati’s diffusion model for oxide dissolution and diffusion into a semi-infinite slab of Nb. The system is governed by the one-dimensional diffusion equation with a source term of a specific form [5]

$$\frac{\partial c(x, t)}{\partial t} = D(T) \frac{\partial^2 c(x, t)}{\partial x^2} + q(x, t, T). \quad (1)$$

The solution to equation (1) is a linear combination of the solution related to the initial interstitial oxygen concentration $v(x, t)$ as and the solution related to oxygen introduced into the surface via oxide dissolution $u(x, t)$ such that $c(x, t) = v(x, t) + u(x, t)$. The solutions to this system are [5]

$$v = \frac{v_0}{\sqrt{\pi D(T)t}} e^{-x^2/(4D(T)t)} + c_\infty \quad (2)$$

$$u = \frac{u_0}{\sqrt{\pi D(T)}} \int_0^t \frac{ke^{-k(T)s}}{\sqrt{t-s}} e^{-x^2/(4D(T)(t-s))} ds. \quad (3)$$

v_0 is the initial interstitial oxygen concentration near the surface and u_0 is related to the oxygen contribution from dissolution of the oxide layer. The rate constant of oxide dissolution and the diffusion coefficient are assumed to exhibit Arrhenius behavior $D(T) = D_0 e^{-E_{ad}/RT}$ and $k(T) = A e^{-E_{ak}/RT}$. c_∞ is the background bulk concentration of interstitial oxygen. From [4] the parameters that describe this process are $v_0 = 3.5$ O at. % nm, $u_0 = 200$ O at. % nm, $E_{ad} = 119.9$ kJ/mol, $D_0 = 0.075$ cm²/s, $E_{ak} = 131$ kJ/mol which corresponds to Nb₂O₅ dissolution, and the frequency factor, $A = 0.9 \times 10^9$ 1/s. Using these values, the landscape of average O concentration in the first 150 nm of Nb can be calculated as a function of vacuum heat treatment temperature and time as shown in Fig. 3. As with nitrogen alloying, the minimization in surface resistance is observed with similar interstitial oxygen concentrations on the order of 1000 ppm [8, 9].

Average O Concentration in First 150 nm

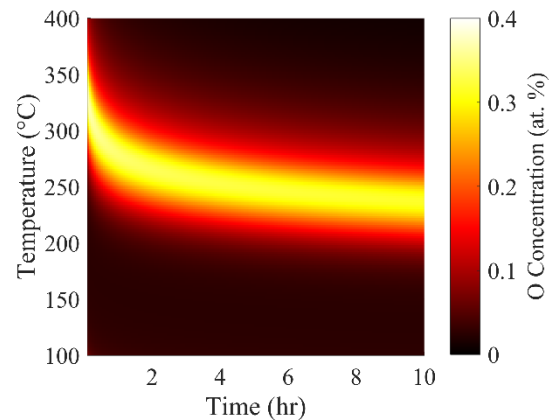


Figure 3: Average oxygen concentration within the first 150 nm colormap using the oxide dissolution and oxygen diffusion values as described in the text.

CONCLUSION

In conclusion, we have shown that the alloying effect observed in the temperature range of 300 – 400 °C for a few hours is primarily associated with oxygen impurities in the RF penetration depth. The effects of oxygen impurity alloying has been confirmed in RF measurements. Using the oxide dissolution and oxygen diffusion model of Ciovati we have predicted the sets of times and

temperatures that should result in an alloying effect using a theory of oxide dissolution and oxygen dissolution.

This oxide dissolution and oxygen diffusion process is an extremely promising development. This process allows for precise tuning of oxygen content by only adjusting the temperature and time the cavity undergoes vacuum heat treatment. Compared to nitrogen alloying (casually known as “doping”), oxygen alloying occurs at temperature where the ingress of other uncontrolled contaminants like C and N is significantly reduced. Furthermore, deleterious phases do not develop upon heat treatment as shown by our RF results after vacuum heat treatment and those in [1, 2]. Unlike cavities subjected to N doping recipes, cavities subjected to O alloying do not require post treatment chemistry. Another benefit is that the oxygen source is already on the cavity. These facts open the possibility to alloy cavities of any geometry.

The relatively low temperatures involved for O-alloying also open alloying to structures where 800°C N alloying heat treatments would be prohibitive. Tailored impurity profiles [13] via a complex temperature ramp vacuum heat-treatment, multiple dissolutions, or tuning the oxygen source preanodization [14] may further add to the versatility of this process allowing full tunability of the electron mean free path from clean to dirty limits. This may be critical for emerging technologies like devices for quantum information systems [15] as well as other applications where the surface interstitials need tuning i.e. thin films [16]. Oxygen alloying related to this work is patent pending under application number 63/189,530.

ACKNOWLEDGEMENTS

This work was co-authored by Jefferson Science Associates LLC under U.S. DOE Contract No. DE-AC05-06OR23177. This material is based on work supported by the U.S. Department of Energy, Office of Nuclear Physics in the Office of Science. The authors are grateful for support from the Office of High Energy Physics, U.S. Department of Energy under Grant No. DE-SC0018918 to Virginia Tech for support of J. Angle.

REFERENCES

- [1] H. Ito *et al.*, “Influence of Furnace Baking on Q-E Behavior of Superconducting Accelerating Cavities,” *Progress of Theoretical and Experimental Physics*, 2021. doi:10.1093/ptep/ptab056
- [2] S. Posen *et al.*, “Ultralow Surface Resistance via Vacuum Heat Treatment of Superconducting Radio-Frequency Cavities,” *Physical Review Applied*, vol. 13, p. 014024, 2020. doi: 10.1103/PhysRevApplied.13.014024
- [3] A. Romanenko *et al.*, “Three-Dimensional Superconducting Resonators at $T < 20$ mK with Photon Lifetimes up to $\tau = 2$ s,” *Physical Review Applied*, vol. 13, no. 3, p. 034032, 2020. doi: 10.1103/PhysRevApplied.13.034032
- [4] E. M. Lechner *et al.*, “RF surface resistance tuning of superconducting niobium via thermal diffusion of native oxide,” *Applied Physics Letters*, vol. 119, no. 8, p. 082601, 2021. doi:10.1063/5.0059464.
- [5] G. Ciovati, “Improved oxygen diffusion model to explain the effect of low-temperature baking on high field losses in niobium superconducting cavities,” *Applied Physics Letters*, vol. 89, no. 2, p. 022507, 2006, doi:10.1063/1.2220059
- [6] H. Tian *et al.*, “The mechanism of electropolishing of niobium in hydrofluoric–sulfuric acid electrolyte,” *Journal of the Electrochemical Society*, vol. 155, no. 9, p. D563, 2008. doi:10.1149/1.2945913
- [7] A. Grassellino *et al.*, “Fermilab experience of post-annealing losses in SRF niobium cavities due to furnace contamination and the ways to its mitigation: a pathway to processing simplification and quality factor improvement,” 2013. doi:10.48550/arXiv.1305.2182
- [8] J. W. Angle *et al.*, “Advances in secondary ion mass spectrometry for N-doped niobium,” *Journal of Vacuum Science & Technology B, Nanotechnology and Microelectronics: Materials, Processing, Measurement, and Phenomena*, vol. 39, p. 024004, 2021. doi:10.1116/6.0000848
- [9] J. Tuggle *et al.*, “Secondary ion mass spectrometry for superconducting radiofrequency cavity materials,” *Journal of Vacuum Science & Technology B, Nanotechnology and Microelectronics: Materials, Processing, Measurement, and Phenomena*, vol. 36, no. 5, p. 052907, 2018. doi: 10.1116/1.5041093
- [10] M. Delheusy *et al.*, “X-ray investigation of subsurface interstitial oxygen at Nb/oxide interfaces,” *Applied Physics Letters*, vol. 92, no. 10, p. 101911, 2008. doi:10.1063/1.2889474
- [11] H. Tian *et al.*, “Surface studies of niobium chemically polished under conditions for superconducting radio frequency (SRF) cavity production,” *Applied Surface Science*, vol. 253, no. 3, pp. 1236-1242, 2006. doi:10.1016/j.apsusc.2006.01.083
- [12] B. King *et al.*, “Measurements of reactive O₂ sticking coefficients and oxidation rates at niobium oxide surfaces,” *Thin Solid Films*, vol. 192, no. 2, pp. 371-381, 1990. doi: 10.1016/0040-6090(90)90080-w
- [13] M. Checchin *et al.*, “High-field Q-slope mitigation due to impurity profile in superconducting radio-frequency cavities,” *Applied Physics Letters*, vol. 117, no. 3, p. 032601, 2020. doi: 10.1063/5.0013698
- [14] M. Biason Gomes *et al.*, “Anodization of niobium in sulphuric acid media,” *Journal of Applied Electrochemistry*, vol. 21, no. 11, pp. 1023-1026, 1991. doi:10.1007/BF01077589
- [15] S. Kutsaev *et al.*, “Niobium quarter-wave resonator with the optimized shape for quantum information systems,” *EPJ Quantum Technology*, vol. 7, no. 1, pp. 1-17, 2020. doi: 10.1140/epjqt/s40507-020-00082-8
- [16] A.-M. Valente-Feliciano, “Superconducting RF materials other than bulk niobium: a review,” *Superconductor Science and Technology*, vol. 29, no. 11, p. 113002, 2016. doi: 10.1088/0953-2048/29/11/113002